

# Edge Detection of Cavity for Identification Tuberculosis Patient in Thorax X-Ray Image

*by* Jufriadif Na`am

---

**Submission date:** 15-May-2020 04:43AM (UTC+0700)

**Submission ID:** 1324441693

**File name:** 2020-TEM\_9\_1\_-Paper.pdf (599.25K)

**Word count:** 3502

**Character count:** 18330

# Edge Detection of Cavity for Identification Tuberculosis Patient in Thorax X-Ray Image

Julius Santony<sup>1</sup>, Johan Harlan<sup>2</sup>, Syafrika Deni Rizki<sup>2</sup>, Yuhandri<sup>1</sup>, Jufriadif Na'am<sup>1</sup>

<sup>1</sup>Universitas Putra Indonesia YPTK, Padang, Indonesia

<sup>2</sup>Universitas Gunadarma, Depok, Indonesia

**Abstract** – Thorax x-ray images are used to identify tuberculous cavities. Sometimes it is difficult to detect the cavity and determine its extent in unprocessed digital image. Image processing serves to help the identification. The method used in this study is Morphological Segmentation and Unsharp Masking. The total number of images which were to be processed was 42, yet only one of them is completely presented and discussed in this article. In all of the post processed images, it can identify tuberculosis cavity and measure its area.

**Keywords** – Edge Detection, Medical Image, Segmentation, X-Ray Image, Tuberculous Cavity.

## 1. Introduction

Tuberculosis patients may present with cavitation, fibrosis or nodular infiltrates, or have a mix of these. [1] The lungs of chronic tuberculosis patients often have cavities [2],[3],[4],[5]. To identify this cavity, thoracal x-ray imaging is used; [6] because such images contain a lot of medical information [7]. However, the benefit of such unprocessed images is quite limited, and it is often difficult to identify the lesion [8]. Time duration needed for the examinations is long, and the results are often unreliable [9]. In thoracal x-ray images, tuberculosis can present a lot of disorders [5].

4

DOI: 10.18421/TEM91-10

<https://doi.org/10.18421/TEM91-10>

**Corresponding author:** Jufriadif Na'am,  
Universitas Putra Indonesia YPTK, Padang, Indonesia.  
Email: [jufriadifnaam@gmail.com](mailto:jufriadifnaam@gmail.com)

Received: 05 October 2019.

Revised: 04 February 2020.

Accepted: 10 February 2020.

Published: 28 February 2020.

© BY-NC-ND © 2020 Julius Santony et al; published by UIKTEK. This work is licensed under the Creative Commons Attribution-NonCommercial-NoDerivs 3.0 License.

The article is published with Open Access at [www.temjournal.com](http://www.temjournal.com)

The disorder is called a lesion, but not all lesions are cavities. Some of the lesions are infiltrates [11]. Cavitation pulmonal images are presented as whitish shadows. But whitish shadows may also indicate other objects, such as the bones and other objects. To precisely identify and calculate the tuberculous cavity area, digital image processing should be performed. In the thoracal x-ray image below, there are several tuberculous cavities as shown by the arrows (Figure 1).

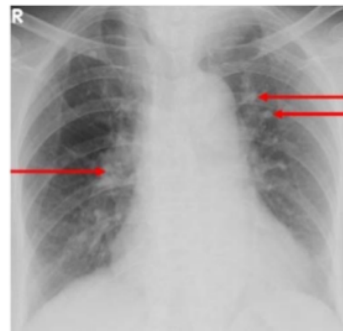


Figure 1. Thorax image that has cavities

Tuberculosis cavity may be circular or slightly elliptical in shape with ill-defined edge. However, the cavity edge has different color with the other parts of the lung. This shows the extent of the wall of the cavity. In terms of imaging intensity, cavities differ from lungs or other objects in the lung. To identify the cavity, a segmentation process is performed to search it within the lung.

X-ray image segmentation is quite useful for the subsequent analysis [12]. Ahmad et al (2015) automatically segmented the lungs with fast execution time [13]. Berg et al (2016) segmented thoracal image to eliminate the bones, thus make it easier to detect fine objects within the lungs [14]. Vital et al (2018) automatically segmented the lungs in thoracal image with high overlap (93.63%) [15].

After the segmentation process, tuberculous cavity can be distinguished from other objects in the thoracal image. Furthermore, a thorough cavity search process was carried out to evaluate the severity of the disease in the thorax. Several studies

have been carried out in order to calculate the area of objects in medical images, e.g. Rodi [17] and Madenda (2013) who calculated the area of nodules in lung Computed Tomography (CT) imaging [16]. Chen (2017) conducted a study of tumor as in CT-scan in [17] to assist the medical analyses [17].

In this paper, we propose edge detection method for identifying tuberculous cavities in the thoracal x-ray images. After identifying the cavity, further feature image processing is carried out, in order to be continued with thorough cavity search. We hope this study is useful in helping medical analysis of tuberculous X-ray imaging. Identification of tuberculosis is important to ensure appropriate therapy [18].

## 2. Materials and Method

There are 42 tuberculous X-ray images to be processed in this study, each has been validated to contain tuberculous cavity by lung clinician. The image processing consisted of several stages using the Matlab Programming application. Every stage is interdependent in a sequential and systematic manner. There is one stage that only supports the overall method, namely pre-processing one. The main steps in these stages are segmentation, feature extraction and feature region. Figure 2 shows the processing steps of this study.

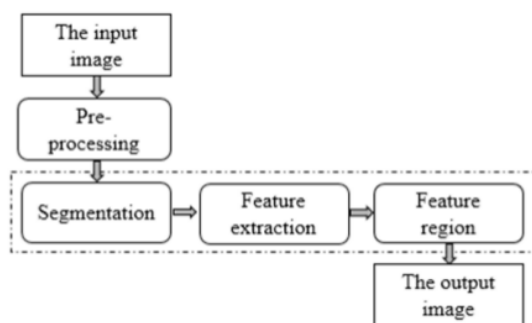


Figure 2. Stage of process in the research

### The input image

Dataset which are analyzed are secondary ones. The x-ray images of thorax are needed [21] the research method. We got the X-ray images processed in this study from Radiology Department of Central General Hospital (RSUP) Dr. M. Djamil Padang, the largest hospital in the West Sumatra Province of Indonesia. These were the X-ray images of patients referred by internal medicine clinician who were checked for tuberculous lesions, devoid of any personal identification information. The number of images that were processed was 42 ones. One of the initial preprocessed images is shown in Figure 1.

The computed radiography device used was the Fuji Film brand with XL II FCR Capsules. The recording technique uses standard pixel density, producing 5 pixels in the width of 1 millimeter (mm). The file format is the Joint Photographic Experts Group (jpg) with the grey scale type. These images have a gray level of 8 bits (28), with grey scale values range from 0 to 255. Each image has a dimension of 1760 x 1760 pixels.

### Pre-processing

Pre-processing is a supporting stage of this research. This stage functions to process the input image before the segmentation process is carried out. The image produced in this stage is very crucial in determining the final image quality produced.

The type of process that is carried out in this stage is manual cropping. [19] This process limits the pixels of the lung as in the thoracal X-ray image. Cropping area is determined by two pixels which served as diagonal end points, namely the first diagonal point and the final diagonal point. The equation used is equation (1).

$$I_{c(w,t)} = Im_{(l2-l1,c2-c1)} \quad (1)$$

$I_{c(w,t)}$  is an image with  $w \times t$  pixel size.  $Im$  is the initial image.  $l1$  is the row position and  $c1$  is the column position at the first diagonal point.  $l2$  is the row position and  $c2$  is the column position of the final diagonal point. The initial pixel position on the cropped image is  $l1$  for the row and  $c1$  for the column ones.

Human lungs consist of 2 parts, namely the left and the right hemisphere. Hence, we [32] form the cropping processes 2 times, first time for the left lung, and second time for the right lung. This preprocessing step as certainty for the unnecessary objects of the X-ray image have been removed.

### Image Segmentation

Segmentation is the process of getting or recognizing a particular object in an image. A good segmentation can accurately and successfully help medical experts in diagnosing disease [20]. This process requires the introduction of certain characteristics of the desired object. Recognizing the objects requires a combination of data obtained from the image to achieve highly accurate results [21]. Data obtained from the image refers to homogeneity, continuity and anatomical texture. Recognition of characteristics can be done by determining similar pixel values in a particular area [22].

The segmentation technique used in this study is Mathematical Morphology (MM), as this technique is still used in image processing. [23] MM is the

process of identifying the form of objects within the region base. In MM there are several operators to process the image according to its characteristics.

The operators used dilation, erosion and gradient in this study. Each operator needs structure of the element (*strel*) as a pixel's stylist in one region. *Strel*

shape used in this study is *strel* (ball, 5, 5). This *strel* is a structuring element with a radius of 5 pixels and height of 5 pixels. The *strel* value is stored in Constanta named *Se*. *-Inf* is the representation of its infinite negative value (negative infinity). The value for each pixel is presented in Figure 3.

-Inf	-Inf	0	0.6248	1.2497	1.8745	1.2497	0.6248	0	-Inf	-Inf
-Inf	0.6248	1.2497	1.8745	2.4994	2.4994	2.4994	1.8745	1.2497	0.6248	-Inf
0	1.2497	1.8745	2.4994	3.1242	3.1242	3.1242	2.4994	1.8745	1.2497	0
0.6248	1.8745	2.4994	3.1242	3.7491	3.7491	3.7491	3.1242	2.4994	1.8745	0.6248
1.2497	2.4994	3.1242	3.7491	4.3739	4.3739	4.3739	3.7491	3.1242	2.4994	1.2497
1.8745	2.4994	3.1242	3.7491	4.3739	4.9987	4.3739	3.7491	3.1242	2.4994	1.8745
1.2497	2.4994	3.1242	3.7491	4.3739	4.3739	4.3739	3.7491	3.1242	2.4994	1.2497
0.6248	1.8745	2.4994	3.1242	3.7491	3.7491	3.7491	3.1242	2.4994	1.8745	0.6248
0	1.2497	1.8745	2.4994	3.1242	3.1242	3.1242	2.4994	1.8745	1.2497	0
-Inf	0.6248	1.2497	1.8745	2.4994	2.4994	2.4994	1.8745	1.2497	0.6248	-Inf
-Inf	-Inf	0	0.6248	1.2497	1.8745	1.2497	0.6248	0	-Inf	-Inf

Figure 3. Pixel values used by *Strel* ball

Dilation operator performs the process of thickening objects in the image. Thickening occurs due to addition of a number of pixels with the same value as the object in the image. The dilation equation is expressed in equation (2). The result of dilation is symbolized by *Id*.

$$Id = Ic \oplus Se \quad (2)$$

Erosion operator performs a process of shrinking objects in an image. Shrinking occurs due to a reduction in the number of pixels with the same value as the object in the image. The erosion equation is expressed in equation (3). The result of erosion is symbolized by *Ie*.

$$Ie = Ic \ominus Se \quad (3)$$

The gradient operator performs a process of reducing the results of the dilation operator with the results of the erosion operator. So, this process will produce object with pixels other than pixels with a value of 0 (black). Pixels with values of 0 become the background of the object in the image. The gradient equation is expressed in equation (4). The gradient image is symbolized by *Ig*.

$$Ig = Id - Ic \quad (4)$$

### Feature Extraction

Feature extraction is the process of taking characteristics of an object based on pixel values in an image [24]. This process will enable us to recognize the pattern of the object. In this process we calculate the number of pixels encountered in an image.

The feature extraction technique used in this study is *unsharp* mask. *Unsharp* mask works to reduce the level of blur by making a mask. The mask value is obtained from the convolution operation of the

sharpen filter in equation (5). Sharpen filter value is represented by *S*. The pixel values are shown in Figure 4.

$$S = \begin{bmatrix} -1 & -1 & -1 \\ -1 & 9 & -1 \\ -1 & -1 & -1 \end{bmatrix}$$

Figure 4. Sharpen filter pixel values

$$M_{(l,c)} = Ie_{(l,c)} - \sum_{i=-a}^a \sum_{j=-b}^b S_{(l,c)} Ie_{(x+l,y+c)} \quad (5)$$

$$a = \frac{m-1}{2} \quad (6)$$

$$b = \frac{n-1}{2} \quad (7)$$

*m* and *n* are the sizes of the sharpen filter. *x* and *y* are image sizes with *l* for row identifiers and *c* for column identifiers. The extraction process is carried out on objects using equation (8), where the resulting image is stored in *Um*.

$$Um = Ie + M \quad (8)$$

To identify the objects, the histogram equalization (HE) process is carried out. This process aims to improve image quality. The way it works is to equalize the grayish histogram value of each pixel based on the pixel value that has the same number of occurrences. The results of this process will further clarify the objects in the image, because objects that are too blurry will disappear, and the objects will obviously become brighter. This process uses equation (9) whose results are stored in *He*.

$$He_{(l,c)} = \frac{kUm_{(l,c)}T}{l.c} \quad (9)$$

*k* is the cumulative histogram of  $Um_{(l,c)}$  and *T* is the threshold with value of  $0 \leq T \leq 255$ .

### Feature Region

Feature region is a process to separate objects from their background in an image. [10] After an object is separated, we can calculate its size. The techniques used in this section are the morphology of the dilation and the function of the *region props* in MatLab. In the process of morphology dilated used *strel* ('disk',2), the pixel values are presented in Figure 5. The function *region props* present the area of the object in the image in a square based on a collection of pixels whose values are close.

0	0	1	0	0
0	1	1	1	0
1	1	1	1	1
0	1	1	1	0
0	0	1	0	0

Figure 5. *Strel* pixel values

The results of this feature region will display an image consisting of pixels with values of 0 as background and the other pixels as the object. Then we can get the size of the object as the result of multiplication of the number of pixels with values greater than 0, with the size area of each pixel. The size area of each pixel has been determined by the computed radiography device.

### 3. Result and Discussion

We acquired thoracal X-ray image of every patient suspected of lung tuberculosis referred to the radiology department. The images are recorded in two media, namely film and digital ones. The results in digital media have been [36] in this study. Among 48 recorded images, only 1 image is presented in this paper.

The sequence of image processing is conducted as shown in Figure 2. Each stage of the process is implemented into the Matlab command. The image produced from each step of the process is presented in Figure 6.

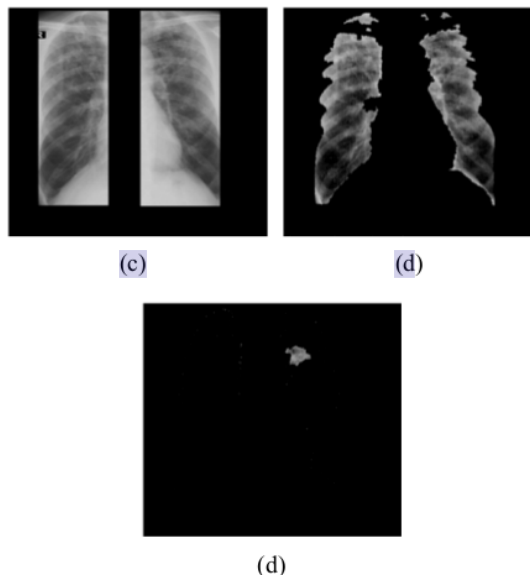
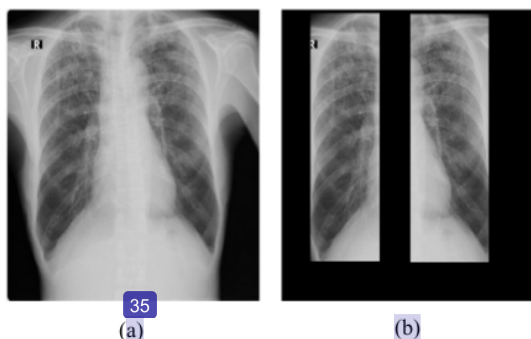


Figure 6. Processing images (a). Input image, (b). Crop result image, (c). Segmentation result image, (d). Image of Feature extraction, (e). Feature region result image

Figure 6 (a) shows the initial image acquired by computed radiography device. Figure 6 (b) shows the result image of cropping process on both sides of the lungs. Crop is done manually in rectangular shape, so there are still many parts that are not lung objects in the result image. Accuracy in determining the first and final diagonal points mainly influences the lung area got in the cropping process.

The result image of segmentation process is shown in Figure 6 (c). The changes of pixel value cannot be visibly observed, but part of the object that has relatively high values (whitish color) has formed the edge of the lung object with relatively low pixel values (blackish color). Because of the growth process (dilated morphology), the size of this object is slightly larger than the actual size, but the difference is not very significant.

In feature extraction process, the pixels outside the edge detection is given values of 0 (black), hence the lung object has been visibly shown. The results of this feature extraction are improved in image quality by the HE process. The result of HE waste clarifies the lung object, as shown in Figure 6 (d). The change is more visible compared to image in Figure 6 (c). But in Figure 6 (d) there are still parts of the lung that are black, which are certainly not cavities.

The last step is the feature region process which localizes the area of cavitation object in Figure 6 (e). The pixels of objects that are not part of the cavities are given the values of 0 (black) in order to distinguish them from the other objects. As the cavity

object is limited to pixels with values other than 0, the size of the cavity area can be calculated.

The final image shows that the only cavity identified is in the left lung hemisphere, while there is no one in the right hemisphere. The number of pixels in the cavity area is 2,656. The radiography manual states that every 1 mm equals 5 pixels, so 1 pixel is 0.2 mm in width. The area of 1 pixel equals to  $0.2 \text{ mm} \times 0.2 \text{ mm}$  or  $0.04 \text{ mm}^2$ . So, the area of the cavity equals to  $2,656 \times 0.04 = 106.24 \text{ mm}^2$ .

#### 4. Conclusion

From the result of processing the thoracic x-ray image, edge detection the tuberculous cavity in the lung of tuberculosis patients can be identified. From the obtained result we can also calculate the area of the cavity; therefore, the proposed method in this study becomes a reference in the subsequent assessment of tuberculosis patients for prevention and treatment.

#### References

- [1]. Hunter, R. L. (2011). Pathology of post primary tuberculosis of the lung: an illustrated critical review. *Tuberculosis*, 91(6), 497-509. Doi: 10.1016/j.tube.2011.03.007.
- [2]. Handa, Dhooria, S., Sehgal, I. S., & Agarwal, R. (2018). Primary cavitary sarcoidosis: A case report, systematic review, a proposal of new diagnostic criteria. *Lung India: Official Organ of Indian Chest Society*, 35(1), 41-46. Doi: 10.4103/lungindia.lungindia.225.17.
- [3]. Li, T.-T., Yan, X., Zhou, T., & Yu, Z.-X. (2018). A challenge: Pulmonary Sclerosing Haemangioma. *Chinese Medical Journal*, 131(19), 2390-2391. Doi: 10.4103/0366-6999.239689.
- [4]. Parkar, A. P., & Kandiah, P. (2016). Differential Diagnosis of Cavitary Lung Lesions. *Journal of the Belgian Society of Radiology*, 100(1), 1-8. Doi: 10.5334/jbr-btr.1202.
- [5]. Petrella, F., Casiraghi, M., Prisciandaro, E., Gherzi, L., & Spaggiari, L. (2019). Incidental diagnosis of pulmonary mycobacteriosis among patients scheduled for lung cancer surgery: results from a series of 39 consecutive operations. *Heliyon*, 5(3), 395. Doi: 10.1016/j.heliyon.2019.e01395.
- [6]. Khlifia, I., Vabre, A., Hočevár, M., Fezzaa, K., Fuzier, S., Roussette, O., & Coutier-Delgosha, O. (2017). Fast X-ray imaging of cavitating flows. *Experiments in Fluids*, 58(157), 3-22. Doi: 10.1007/s00348-017-2426-7.
- [7]. Hellbach, K., Baehr, A., De Marco, F., Willer, K., Groman, L. B., Herzen, J., ... & Rummeny, E. J. (2018). Depiction of pneumothoraces in a large animal model using x-ray dark-field radiography. *Scientific reports*, 8(1), 1-8. Doi: 10.1038/s41598-018-20985-y.
- [8]. ITO, K. (2005). Limits of chest X-ray investigation in the diagnosis of recurrent pulmonary tuberculosis. *Kekkaku (Tuberculosis)*, 80(7), 521-526. Doi: 10.11400/kekkaku1923.80.521.
- [9]. Jaeger, S., Karagyris, A., Candemir, S., Folio, L., Siegelman, J., Callaghan, F., Xue Z., Palaniappan K., Singh R., Antani S., Thoma G., Wang Y., Lu P., McDonald, C. J. (2014). Automatic tuberculosis screening using chest radiographs. *IEEE Transactions on Medical Imaging*, 33(2), 233-245. Doi: 10.1109/TMI.2013.2584099.
- [10]. Sumijan, Madenda, S., Harlan, J., & Wibowo, E. P. (2017). Hybrids Otsu method, feature region and mathematical morphology for calculating volume hemorrhage brain on CT-scan image and 3D reconstruction. *Telkomnika (Telecommunication Computing Electronics and Control)*, 15(1), 283-291. Doi: 10.12928/TELKOMNI.v15i1.3146.
- [11]. Santony, J., & Naam, J. (2016). Infiltrate Object Extraction in X-ray Image by using Math-Morphology Method and Feature Region Analysis. *International Journal on Advanced Science, Engineering and Information Technology*, 6(2), 239-244. Doi: 10.18517/ijaseit.6.2.763.
- [12]. Schlüter, S., Sheppard, A., Brown, K., & Wildenschild, D. (2014). Image processing of multiphase images obtained via X-ray microtomography: a review. *Water Resources Research*, 50(4), 3615-3639. Doi: 10.1002/2014WR015256.
- [13]. Ahmad, W. S. H. M. W., Zaki, W. M. D. W., & Fauzi, M. F. A. (2015). Lung segmentation on standard and mobile chest radiographs using oriented Gaussian derivatives filter. *Biomedical engineering online*, 14(1), 20. Doi: 10.1186/s12938-015-0014-8.
- [14]. von Berg, J., Levrier, C., Carolus, H., Young, S., Saalbach, A., Laurent, P., & Florent, R. (2016, April). Decomposing the bony thorax in X-ray images. In *2016 IEEE 13th International Symposium on Biomedical Imaging (ISBI)* (pp. 1068-1071). IEEE. Doi: 10.1109/ISBI.2016.7493450.
- [15]. al, D. A., Sais, B. T., & Moraes, M. C. (2018). Robust pulmonary segmentation for chest radiography, combining enhancement, adaptive morphology and innovative active contours. *Research on Biomedical Engineering*, 34(3), 234-245. Doi: 10.1590/2446-4740.180035.
- [16]. diah, & Madenda, S. (2013). Ekstraksidan Perhitungan Luas Nodul Citra CT Scan KankerParu. *Konferensi Nasional Sistem Informatika 2013. STMIK migora Mataram*, 510-515. 14-16 Pebruari 2013.
- [17]. Chen, Y. T. (2017). A novel approach to segmentation and measurement of medical image using level set methods. *Magnetic Resonance Imaging*, 39, 175-193. Doi: 10.1016/j.mri.2017.02.008.
- [18]. Jeong, Y. J., Lee, K. S., & Yim, J.-J. (2017). The diagnosis of pulmonary tuberculosis: a Korean perspective. *Precision and Future Medicine*, 1(2), 77-87. Doi: 10.23838/pfm.2017.00114.

- [19]. handri, S. M., & Wibowo, E. P. (2017). Karmilasari, "Object Feature Extraction of Songket Image Using Chain Code Algorithm," *Int. J. Adv. Sci. Eng. Inf. Technol.*, 7(1), 235-241. Doi: 10.1107/ijaseit.7.1.1479.
- [20]. Na'am, J., Harlan, J., Madenda, S., Santony, J., & Suharinto, C. (2018). Detection of Proximal Caries at The M<sup>29</sup> Teeth Using Edge Enhancement Algorithm. *International Journal of Electrical and Computer Engineering (IJECE)*, 8(5), 3259-3266.
- [21]. Chijindu, V. C., Udeze, C. C., Ahaneku, M. A., & Anoliefo, E. C. (2018). Detection of Prostate Cancer Using Radial/Axial Scanning of 2D Trans-rectal Ultrasound Images. *Bulletin of Electrical Engineering and Informatics*, 7(2), 222-229. Doi: 10.11591/eei.v7i2.727.
- [22]. Hasan, A. M. (2018). A Hybrid Approach of Using Particle Swarm Optimization and Volumetric Active Contour without Edge for Segmenting Brain Tumors in MRI Scan. *Indonesian Journal of Electrical Engineering and Informatics (IJEI)*, 6(3), 292-300. Doi: 10.11591/ijeie.v6i3.592.
- [23]. Ledda, A. (2007). *Mathematical Morphology in Image Processing*. Thesis.
- [24]. Oktiana, M., Arnia, F., Away, Y., & Munadi, K. (2018). Features for cross spectral image matching: A survey. *Bulletin of Electrical Engineering and Informatics*, 7(4), 552-560. Doi: 10.11591/eei.v7i4.843.

# Edge Detection of Cavity for Identification Tuberculosis Patient in Thorax X-Ray Image

## ORIGINALITY REPORT

24%

SIMILARITY INDEX

17%

INTERNET SOURCES

19%

PUBLICATIONS

14%

STUDENT PAPERS

## PRIMARY SOURCES

1	<a href="https://medium.com">medium.com</a> Internet Source	1%
2	Submitted to dBs Music Student Paper	1%
3	<a href="http://www.imt.kit.edu">www.imt.kit.edu</a> Internet Source	1%
4	<a href="http://www.sarjournal.com">www.sarjournal.com</a> Internet Source	1%
5	<a href="http://harlan_johan.staff.gunadarma.ac.id">harlan_johan.staff.gunadarma.ac.id</a> Internet Source	1%
6	<a href="http://biomedical-engineering-online.biomedcentral.com">biomedical-engineering-online.biomedcentral.com</a> Internet Source	1%
7	M. M. Yamunadevi, S. Siva Ranjani. "Efficient segmentation of the lung carcinoma by adaptive fuzzy–GLCM (AF-GLCM) with deep learning based classification", Journal of Ambient Intelligence and Humanized Computing, 2020	1%



8

Andrew, Matthew, Branko Bijeljic, and Martin Blunt. "Reservoir Condition Pore Scale Imaging of the Capillary Trapping of CO2", Energy Procedia, 2014.

Publication

---

9

[eprints.qut.edu.au](http://eprints.qut.edu.au)

Internet Source

---

10

Dae-han Kim, Hyun-chong Cho. "Superpixel Approach in Computer-Aided Detection System of Dental Cavities in X-Ray Images", Journal of Electrical Engineering & Technology, 2020

Publication

---

11

Thrivikram Bathini, Baswaraj Gadgay. "Hybrid enhanced ICA & KSVM based brain tumor image segmentation", Indonesian Journal of Electrical Engineering and Computer Science, 2018

Publication

---

12

Submitted to University of California, Los Angeles

Student Paper

---

13

[uthealth.influent.utsystem.edu](http://uthealth.influent.utsystem.edu)

Internet Source

---

14

Submitted to Universiti Teknologi Malaysia

Student Paper

---

1%

1%

1%

1%

1%

1%

1%

15

[jtiik.ub.ac.id](http://jtiik.ub.ac.id)

Internet Source

1%

16

Saad Jahangir, Evert C. Wagner, Robert F. Mudde, Christian Poelma. "Void fraction measurements in partial cavitation regimes by X-ray computed tomography", International Journal of Multiphase Flow, 2019

Publication

1%

17

"Medical Image Computing and Computer Assisted Intervention – MICCAI 2018", Springer Science and Business Media LLC, 2018

Publication

1%

18

Maulisa Oktiana, Takahiko Horiuchi, Keita Hirai, Khairun Saddami, Fitri Arnia, Yuwaldi Away, Khairul Munadi. "Cross-spectral iris recognition using phase-based matching and homomorphic filtering", Heliyon, 2020

Publication

1%

19

Submitted to Griffith University

Student Paper

1%

20

D. Palani, K. Venkatalakshmi. "An IoT Based Predictive Modelling for Predicting Lung Cancer Using Fuzzy Cluster Based Segmentation and Classification", Journal of Medical Systems, 2018

Publication

1%

21 Jufriadif Na'am, Julius Santony, Yuhandri Yuhandri, Sumijan Sumijan, Gunadi Widi Nurcahyo. "Enlarge Medical Image using Line-Column Interpolation (LCI) Method", International Journal of Electrical and Computer Engineering (IJECE), 2018  
Publication 1%

---

22 Submitted to University of Leeds  
Student Paper 1%

---

23 Akhmad Fadjeri, Arief Setyanto, Mei P. Kurniawan. "Pengolahan Citra Digital Untuk Menghitung Ekstrasi Ciri Greenbean Kopi Robusta Dan Arabika (Studi Kasus: Kopi Temanggung)", Jurnal Teknologi Informasi dan Komunikasi (TIKomSiN), 2020  
Publication <1%

---

24 [rbejournal.org](http://rbejournal.org)  
Internet Source <1%

---

25 [journals.viamedica.pl](http://journals.viamedica.pl)  
Internet Source <1%

---

26 [www.mitrariset.com](http://www.mitrariset.com)  
Internet Source <1%

---

27 Submitted to University of Edinburgh  
Student Paper <1%

---

28 Piotr Ksiazak, William Farrelly, Kevin Curran. <1%

"chapter 1 A Lightweight Authentication and Encryption Protocol for Secure Communications Between Resource-Limited Devices Without Hardware Modification", IGI Global, 2018

Publication

29

[papers.ssrn.com](https://papers.ssrn.com)

Internet Source

<1%

30

Submitted to University of Kent at Canterbury

Student Paper

<1%

31

Submitted to Syiah Kuala University

Student Paper

<1%

32

[www.scielo.br](http://www.scielo.br)

Internet Source

<1%

33

Submitted to Lane Technical College  
Preparatory High School

Student Paper

<1%

34

Yao-Tien Chen. "A novel approach to segmentation and measurement of medical image using level set methods", Magnetic Resonance Imaging, 2017

Publication

<1%

35

[ar.scribd.com](https://ar.scribd.com)

Internet Source

<1%

36

"Applied Computing to Support Industry: Innovation and Technology", Springer Science

<1%

---

37 Submitted to University of Bradford <1%  
Student Paper

---

38 [ejournal.uin-suska.ac.id](http://ejournal.uin-suska.ac.id) <1%  
Internet Source

---

39 Francesco Petrella, Monica Casiraghi, Elena Prisciandaro, Lorenzo Gherzi, Lorenzo Spaggiari. "Incidental diagnosis of pulmonary mycobacteriosis among patients scheduled for lung cancer surgery: results from a series of 3224 consecutive operations", Heliyon, 2019 <1%  
Publication

---

40 Bounegta Nadia, Bassou Abdessalam, Beladgham Mohamed. "Eyelids, eyelashes detection algorithm and houghtransform method for noise removal in iris recognition", Indonesian Journal of Electrical Engineering and Computer Science, 2020 <1%  
Publication

---

Exclude quotes Off

Exclude matches Off

Exclude bibliography Off